Calibration approaches in Multi-Node Antenna Characterization Setups

Coesoij, R.A.; Musters, F.A.; Roos, D.; van Velden, T.; Spirito, M.

DOI
10.1109/ARFTG56062.2023.10148881

Publication date
2023

Document Version
Final published version

Published in
Proceedings of the 2023 100th ARFTG Microwave Measurement Conference (ARFTG)

2023 100th ARFTG Microwave Measurement Conference (ARFTG) | 978-1-6654-7494-8/23/$31.00 ©2023 IEEE | DOI: 10.1109/ARFTG56062.2023.10148881

Calibration approaches in Multi-Node Antenna Characterization Setups

R.A. Coesoij, F.A. Musters, D. Roos, T. van Velden, M. Spirito

Delft University of Technology, 2628 CD, Delft, The Netherlands

***Abstract* — In this work we present calibration approaches aimed at mitigating the measurement error in testbenches featuring multiple sensor-nodes and operating over-the-air. Such errors can arise from fluctuations in component responses and mechanical tolerances of the setup. The calibration approaches are detailed for the case of the Antenna Dome measurement setup previously presented by the authors.**

In the current implementation, the Antenna Dome employs multiple dual linearly-polarized scalar sensing nodes, to enable real-time 2D (theta and phi) radiation pattern acquisition. The variation of the electrical response among the different sensing elements as well as their position, with respect to the nominal one, due to the mechanical tolerances, introduce systematic error in the generated radiation patterns.

Over-the-air procedures to linearize the power conversion asymmetry within the dually polarized nodes as well as the linearity response across them are described. Proposed approach provides a reduction of the angular dependent error within ±0.5 dB across the various nodes. Moreover, to minimize the impact of mechanical deviations an over-the-air method is described to transfer the sensor coordinates from the mechanical reference system to the antenna under test one.

***Index Terms* — [multi-probe, antenna measurement, over-the-air, scalar radiation pattern, dual-polarized, polarization, detector].**

I. Introduction

The 5G New Radio (NR) access points aimed for the FR2 band are going to require fast and reliable over-the-air (OTA) testing approaches to accelerate their deployment and market penetration. The characterization of active elements and antenna front-end needs to be carried on the entire unit to identify potential reflection and element-to-element non-linear effects, over multiple beam steering angles to comply with industry requirements [1,2].

The Antenna Dome [3] was developed to enable real-time 2D (theta and phi) radiation pattern acquisition by removing all mechanical movements and employing a large number of dual-polarized scalar power sensing nodes. Compared to the work presented in [3], the dome skeleton is now realized with a geodesic structure (see Fig. 1a) to improve the structure mechanical stability and scalability. Each sensing node is composed of two scalar detectors, each linearly polarized and oriented 90º in respect to each other. This allows, summing their individual received power, to obtain constant power detection, independent of the incoming polarization. With the knowledge of the angular position (theta and phi) of each sensor in the dome, allows to directly reconstruct the 2D radiation pattern using conventional interpolation schemes. Nevertheless, the relative electrical response of the detectors, within a sensor node unit and across the different nodes, in conjunction with the mechanical tolerances (i.e., imperfections) of the node position placement result in systematic error in the reconstructed patterns.

To compensate for these errors, this work describes two over-the-air calibration procedures to minimize both the offsets electrical response and deviation from the nominal position.

The paper is organized as follows: In Section II the configuration of the Antenna Dome is explained with respect to previous work. Section III introduces the approaches to minimize position inaccuracies with respect to the AUT reference system. After, the non-idealities i.e., imbalances, within a single node are analyzed and Section IV presents the compensation techniques, at node level and across nodes of the Antenna Dome.

II. A Distributed Sampling Environment – The Antenna Dome

The Antenna Dome in its current implementation, is configured using 26 dual-polarized sensing nodes distributed as shown in Fig. 1b. Twenty sensing nodes are placed on the joints connecting the aluminum profiles. The boresight node and the remaining five sensing nodes are placed in the center of the five hexagons in the upper part the geodesic dome. The node with the lowest elevation is placed at 31.6 degrees, considering the boresight node at an elevation of 90 degrees. The distance R between the AUT and the sensing nodes is 50 cm.

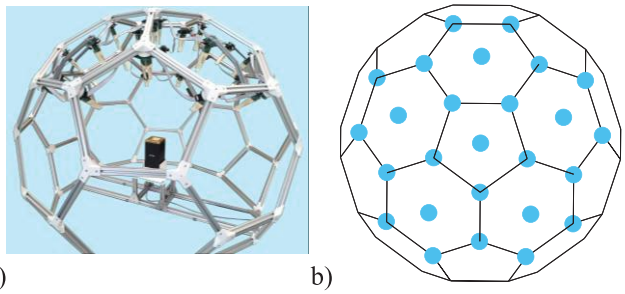

a) b)

Fig. 1: a) Antenna Dome with geodesic dome skeleton, b) Top view node nominal configuration in respect to the mechanical assembly.

III. Relative Calibration Methods

This section treats the techniques to compensate the imbalances arising from the deviations from the nominal sensor position in the setup and the varying responsivity across the detectors.

A. Optical Positioning

The power measured by each sensor node needs to be plotted in a spatial domain to reconstruct (via interpolation) the antenna radiation pattern. In systems employing a large number of nodes, an efficient approach to associate each specific node to its spatial location needs to be implemented. In the Antenna Dome an optical calibration system is used to perform this function.

To realize this, each node sequentially activates an LED placed on its control board and via optical mapping, the nearest grid point, shown in Fig 1b with blue highlights, on the geodesic dome is selected as the location of the node under test.

B. Mechanical Positioning

To further improve positional accuracy of the sensing nodes and therefore the representation of the radiation pattern, an optimization procedure employing node response is performed. For each node, a grid, in the AUT mechanical control system, is defined. A search to find the maximum power for each node is then performed, and used for the alignment. The increase in received power after alignment is shown in Fig. 2a. The corrected positions of the nodes are shown in red in Fig. 2b.

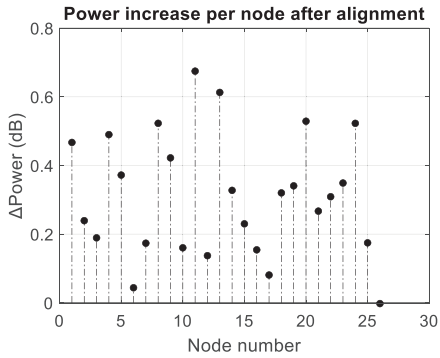

a)

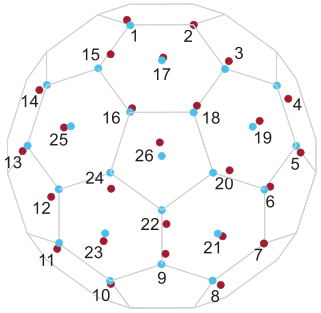

b)

Fig. 2: a) Power variation (increase) after alignment for all nodes; b) Initial positions (blue) and adjusted positions (red).

To implement the method, a two-axis Newmark GM-6 gimbal positioner is placed in the center of the dome to enable precise positioning within the reference coordinate system of the dome. The specified accuracy and resolution of the positioner is ±0.02/0.001 degrees, respectively.

Initially, the positioner is set to the ideal coordinates of the sensing node under test. After, a coarse grid is scanned over which the power is measured. The measured power of both polarizations are summed. Maximum power is measured when both the AUT and receiving antenna are aligned. This measurement can be used in conjunction with the optical positioning method to more precisely define the position of the sensing node with respect to its ideal geometrical/mechanical reference position.

C. Normalization across sensor units

After the improved location of the sensors are identified, the power response of the various sensors are aligned. Differences in responsivity (i.e., output voltage over the input RF power) can arise from variation in technology of the various units, and can be corrected using a frequency and power dependent look-up table. Using the coordinate locations identified in the previous setup, a line-of-sight measurement is performed for each of the nodes, sweeping the CW power of the source generator, provided to a standard horn fitted in the two-axis Newmark GM-6 gimbal positioner. The result of the raw measurement (i.e., before correction) is shown in Fig 3a.

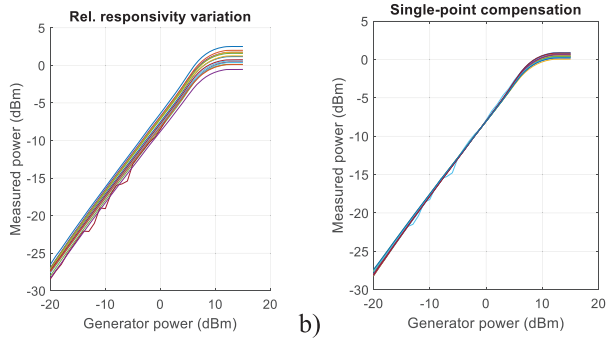

a) b)

Fig. 3: Over-the-air power sweep measurement, a) before and b) after correction

To reduce the relative offsets between the nodes (ca. 4 dB across the nodes), a single- point correction is performed and the result is shown in Fig 3b. This calibration can be extended to multiple frequencies. Additionally, to minimize the errors between the nodes over a larger dynamic range, multi-point correction terms can be included in this compensation.

IV. Polarization of the Detector Cell

The Antenna Dome employs dual-polarized RMS detectors directly embedded in the high frequency antenna board, as shown in Fig. 4. The usage of two separate detectors introduce asymmetries in the total power received which are discussed in detail in this section.

Fig. 4: Dual polarized sensing unit employed in the Antenna Dome.

A. *Dual linearly-polarized antenna*

The sensing nodes are configured as shown in Fig. 4 using two antipodal Vivaldi antennas as described in [2]. The antennas are placed orthogonally to each other in order to detect both polarizations simultaneously. Nevertheless, due to components response spread, the output voltage of each of the detector can be different even when the same power is applied to each polarization.

To study this effect a measurement at a fixed frequency and power is performed in which a standard gain horn antenna is rotated 360 degrees in steps of 1 degree, using a two-axis gimbal. The power received by each sensor and the summation between the two sensor are shown in Fig. 5.

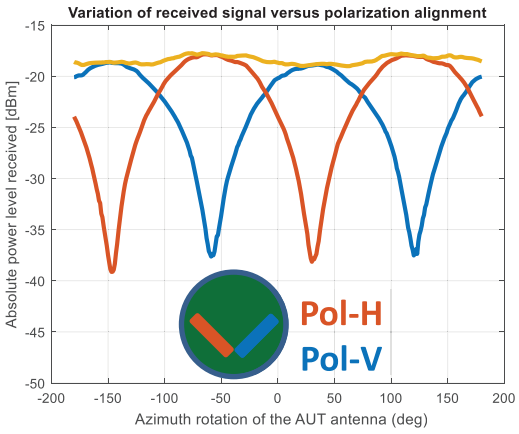

Fig. 5: Power received versus angle of the AUT for the two polarization of the broadside node.

In a perfectly balanced case, the yellow line of Fig. 5 should provide a constant value versus angle [4]. However, due to component variations the response of each sensing unit will be different. The mismatch from the constant power response can be used as a correction factor to balance the power received for that specific sensor, as will be shown in the next section.

B. *Polarization variation of multiple nodes*

In order to perform the characterization procedure described in Fig. 5 to all the nodes of the Antenna Dome, a three-axis gimbal would be required. This motorized unit was not available and is not often used in antenna chambers due to the larger volume occupancy. For this reason, a reduced set of sampling points was acquired using a 3D printed fixture. This enables the AUT to be manually rotated in steps of 22.5 degrees in a third axis of rotation as shown in Fig 6.

The measurement is automated and is performed by setting the CW generator at a fixed frequency and power level. The positioner is set to point the reference antenna to each individual node, for each of the five angles shown in Fig. 6.

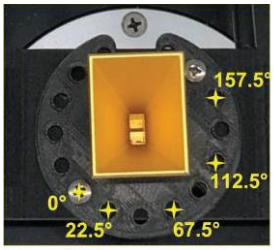

Fig. 6: WR-28 Standard gain horn antenna (27.4mm x 21.9mm) and fixture providing the third axis of rotation.

The measurement is repeated and the measured power versus the angular rotation of the polarization is acquired. The sampled data point are processed via curve fitting [5] to reconstruct the correction factor versus angle, as was done with the boresight node. This procedure is shown in Fig. 7.

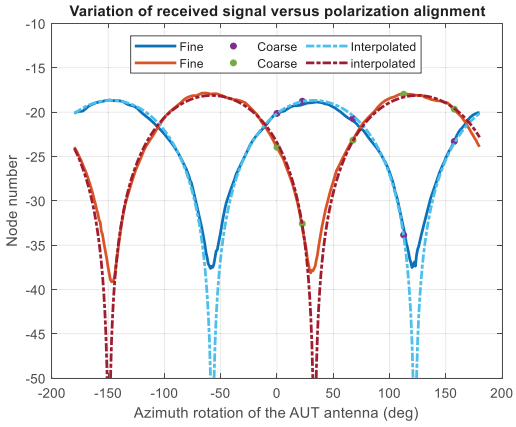

Fig. 7: Comparison between interpolated data using sampling points (Coarse) and measured data (Fine) for the boresight node.

The interpolated data is in good agreement with the fine measurement data. The maximum error between the fitted data and measurement data is 0.5 dB. Employing the reconstructed characteristics allows to extract an angle dependent correction factor similar to the boresight node, even while using the two-axis gimbal.

C. *Relative polarization correction*

The polarization characteristics discussed in the previous section are used to determine the required correction factor to minimize the variation per sensing node.

The error correction is applied as follows: first the angle of the AUT in respect to the Dome sensing nodes is identified from the boresight node, then the correction factor is identified for any node in the Dome and the sign inverse value is added to the sum power over the two polarization, as shown in Fig. 8.

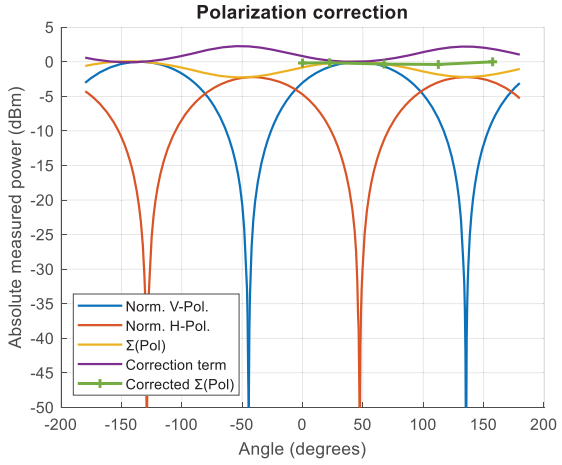

Fig. 8: Compensation of the polarization variation. The blue and orange curves are the fitted normalized curves based on the measurement of sampled points. The sum of the normalized curves is represented as the yellow curve. Consequently, the inverse is determined and shown as the purple curve – representing the correction term. The green curve represents the residual variation after correction.

The method is then applied to the remaining 25 nodes, to compensate for the relative errors between the various sensing nodes. The resulting variations between the multiple nodes, before and after correction are shown in Fig. 9.

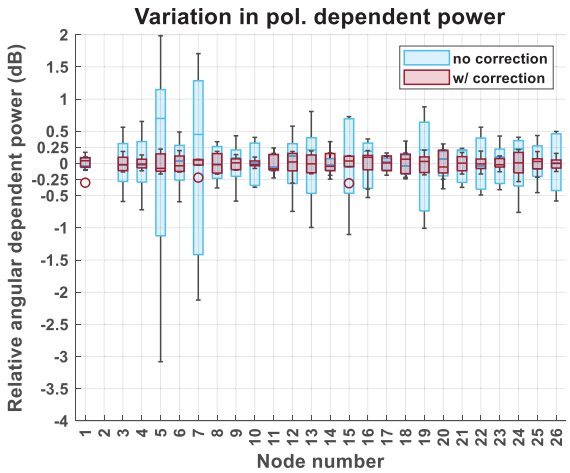

Fig 9: Spread in received power for the various angular measurements. Before (blue) and after (dark red) compensation.

The data represents the measured power of each node, for the various angular setting of the horn under test, i.e., 5 locations of Fig. 6. The average values of the spread are normalized to 0 dB to evaluate the compensation technique. When the starting error spreads is smaller than ±0.5 dB the compensation technique is less effective. For example, node 14 in Fig. 9. When the polarization errors without compensations are larger than ±0.5 dB the procedure strongly reduces this imbalance.

V. Conclusion

This work addresses several calibration approaches that can be applied to testbenches featuring multiple sensor-nodes and operating over-the-air. In specific, positioning, responsivity and polarization errors. The current multi-node setup included a few non-idealities. Including an environment sensitive to reflections, influencing the presented measurement results and compensation techniques.

The alignment and responsivity calibration approaches reduced the spread in the sampled power (over-the-air) across sensors, to well below 1dB. Moreover, the results of polarization compensation technique shows a consistent improvement when a large imbalance is present and provides a limit for the compensation at around 0.5 dB.

The presented techniques provide insight in scalar calibration for multi-node antenna characterization setups to enable real-time scalar acquisition of the radiation pattern for 5G mm-wave phased array antennas.

References

[1] M. Maggi *et al*., "Millimeter-Wave Phased Arrays and Over-the-Air Characterization for 5G and Beyond: Overview on 5G mm-Wave Phased Arrays and OTA Characterization," in *IEEE Microwave Magazine*, vol. 23, no. 5, pp. 67-83, May 2022, doi: 10.1109/MMM.2022.3148328.

[2] "IEEE Recommended Practice for Antenna Measurements," in *IEEE Std 149-2021 (Revision of IEEE Std 149-1977)* , vol., no., pp.1-207, 18 Feb. 2022, doi: 10.1109/IEEESTD.2022.9714428..

[3] F. A. Musters, R. A. Coesoij, M. D. Migliore, F. Schettino and M. Spirito, "The Antenna Dome Real-Time Distributed Antenna Pattern Characterization System," *2021 97th ARFTG Microwave Measurement Conference (ARFTG)*, 2021, pp. 1-5, doi: 10.1109/ARFTG52261.2021.9640079.

[4] C. A. Balanis, "2.12.2 Polarization Loss Factor and Efficiency," in *Antenna Theory: Analysis and Design Edition*, Hoboken, New Jersey John Wiley & Sons, 2016,.

[5] MathWorks, (2022). *Curve Fitter Toolbox (R2022a)*. Retrieved October 14, 2022 from www.mathworks.com/help/curvefit/curvefitter-app.html